Supporting Information

Diril et al. 10.1073/pnas.1115201109

SI Materials and Methods

Primers, Genotyping, and Real-Time PCR. For PCR genotyping of cyclin-dependent kinase 1 (Cdk1), wild-type, FLOX, and null alleles, primers Pr1, Pr2, and Pr3 (Table S1) were used at 1 μM final concentration. Briefly, cells or tissue pieces to be genotyped were lysed by boiling in lysis solution (25 nM NaOH and 0.2 mM EDTA) for 20–30 min to extract genomic DNA (1). Alkaline pH was neutralized by the addition of an equal volume of neutralization buffer (40 mM Tris·HCl). One microliter of the resultant genomic DNA solution was used as a template in a 20-μL volume of PCR with 0.5 units of MangoTaq polymerase (Bioline). Thirty-five PCR cycles with 30-s denaturation at 94 °C, 30-s annealing at 68 °C, and 30-s extension at 72 °C were performed to amplify different alleles of Cdk1, resulting in a band of 159 bp ($Cdk1^{WT}$), 255 bp ($Cdk1^{FLOX}$), or 389 bp ($Cdk1^{NULL}$).

Quantification of mRNA levels at different time points of cell-cycle entry in synchronized $Cdk1^{FLOX}$ and $Cdk1^{NULL}$ mouse embryonic fibroblasts (MEFs) was measured by real-time PCR using a Rotor-Gene 6000 instrument (Corbett Life Science) and the Maxima SYBR Green kit (Fermentas). Some of the primers used were designed in house, whereas others were purchased from SABiosciences (Table S2).

Cdk1 Conditional Knockout Mice and Other Transgenic Lines. To generate the $Cdk1^{FLOX}$ allele, the neomycin cassette was removed by crossing Cdk1 conditional knockout mice with β-actin–Flpe transgenic mice (2) [strain name: B6.Cg-Tg(ACTFLPe)9205Dym/J; stock no.: 005703; The Jackson Laboratory]. The $Cdk1^{NULL}$ allele was generated by crossing $Cdk1^{FLOX}$ mice with β-actin–Cre transgenic mice (3) [strain name: FVB/*N*-Tg(ACTB-cre)2Mrt/J; stock no.: 003376; The Jackson Laboratory]. Liver-specific Cdk1 knockout was accomplished by crossing $Cdk1^{FLOX}$ mice with albumin-Cre transgenic mice (4). 4-Hydroxytamoxifen (4-OHT)-inducible conditional knockouts were created by crossing with either Cre-Esr1 (5) [strain name: B6.Cg-Tg(CAG-cre/Esr1*)5Amc/J; stock no.: 004682; The Jackson Laboratory] or Rosa26-CreERT2 transgenic mice (6).

Mice were housed under standard conditions with food and water available ad libitum and maintained on a 12-h light/dark cycle. Mice were fed a standard chow diet containing 6% crude fat and were treated humanely in compliance with the Institutional Animal Care and Use Committee guidelines.

Blastocyst Isolation and Image Analysis. Timed matings between $Cdk1^{+/NULL}$ mice were set up and, at 3 d after the observation of a vaginal plug (E3.5), females were euthanized to isolate blastocysts. Embryos were flushed out of the uterine horns (7) and collected in DMEM supplemented with 10% FCS and 5 μg/mL of Hoechst 33342 dye (Invitrogen) to monitor the nuclei. Individual embryos were placed in 20-μL droplets of same medium, and serial *Z*-stacks of blastocysts were acquired under 20× magnification with an Axiovert Imager Z1 microscope (Carl Zeiss). Embryos were recovered and placed in 5 μL of lysis solution, boiled 20 min, and neutralized by the addition of 5 μL of neutralization buffer, and genotyping PCRs were performed as described above.

Western Blot Analysis, Immunoprecipitation, and Kinase Assays. Cells and tissues were lysed in EBN buffer [80 mM β-glycerophosphate (pH 7.3), 20 mM EGTA, 15 mM $MgCl_2$, 150 mM NaCl, 0.5% Nonidet P-40, 1 mM DTT, and protease inhibitors (20 μg/mL each of leupeptin, chymostatin, and pepstatin; EI8, EI6, and EI10; Chemicon)] for 20 min with constant shaking at 1,200 rpm. Lysates were centrifuged for 30 min at 18,000 × *g* at 4 °C, and supernatants were snap-frozen in liquid nitrogen and stored at −80 °C. Ten micrograms of protein extracts were separated on 10% or 12.5% polyacrylamide gels, transferred onto PVDF membranes (IPVH0010; Millipore) using a semidry system, and blocked in Tris-buffered saline with 0.1% Tween 20 and 5% nonfat dry milk (1706404; Bio-Rad). Blots were probed with the appropriate primary antibodies overnight at 4 °C, followed by secondary goat anti-mouse (0031432; Pierce) or anti-rabbit (0031462; Pierce) antibodies conjugated to horseradish peroxidase and developed using enhanced chemiluminescence (NEL105001EA; PerkinElmer). All antibodies used in Western blots are commercially available: mouse anti-Cdk1 (sc-54; Santa Cruz Biotechnology), mouse anti-Cdk2 (sc-6248; Santa Cruz Biotechnology), rabbit anti–phospho-Cdk1–Tyr15 (9111; Cell Signaling), rabbit anti-cyclin A2 (sc-596; Santa Cruz Biotechnology), mouse anti-cyclin A2 (AHF0022; Biosource), mouse anti-cyclin B1 (4135; Cell Signaling), mouse anti-p21 (sc-6246; Santa Cruz Biotechnology), mouse anti-p27 (610242; BD Transduction), mouse anti-Hsp90 (610419; BD Transduction), goat anti-actin (sc-1616; Santa Cruz Biotechnology), and mouse anti-Cre recombinase (MAB3120; Millipore).

Affinity purification/immunoprecipitation and kinase assays were performed as described previously (8) with minor modifications. Briefly, 100–250 μg of protein extract was incubated with beads decorated with Suc1 (14-132; Upstate Biotechnology) or antibodies against Cdk1 (sc-54; Santa Cruz Biotechnology), Cdk2 (8), cyclin A2 (sc-751; Santa Cruz Biotechnology), and cyclin B1 (8) overnight at 4 °C in EBN buffer supplemented with 1 mg/mL ovalbumin (A5503; Sigma). Antibodies were precoupled to protein A (11719408001; Roche) or protein G (11719416001; Roche) agarose beads. After two washes in EBN buffer and one wash in EB buffer (EBN without Nonidet P-40), the precipitated proteins were either resolved by SDS/PAGE for Western blot analysis or used in kinase assays to determine the levels of kinase activity against the substrate histone H1 (11004875001; Roche). Kinase assays were performed by incubating the immunoprecipitated proteins on beads in EB buffer (EBN without Nonidet P-40) with 10 mM DTT, 15 μM ATP, 5 μCi [γ-^{32}P]ATP (NEG502A; PerkinElmer) and 1.5 μg of histone H1 for 30 min at room temperature, inactivation with SDS/PAGE sample buffer, electrophoresis on polyacrylamide gel, fixation and staining in Bismarck Brown/Coomassie blue, and quantification of incorporated radioactivity with a phosphoimager (FLA-7000; Fujifilm).

Purified recombinant full-length Cdk1/cyclinA2, Cdk1/cyclinB1, and Cdk2/cyclinA2 were purchased from Cell Signaling (7477, 7518, and 7521).

Cell Culture and FACS Analysis. All cell-based experiments were performed with primary MEFs isolated from three different embryos from the same litter with the $Cdk1^{FLOX/FLOX}$;$Cre\text{-}Esr1^{TG/TG}$ genotype. Presence of two copies of the Cre-Esr1 transgene was confirmed by real-time PCR analysis. All experiments were done with passage 1 cells.

For 3T3 assays, 300,000 primary MEFs were plated in 10-cm dishes in duplicate in the presence or absence of 20 ng/mL 4-OHT. Every 3 d, cells were trypsinized and counted, and 300,000 cells (or when cell number was less than 300,000, all remaining cells) were replated.

For alamarBlue proliferation assays, 1,500 cells were plated in 96-well plates in five replicates, with or without prior 4-OHT treatment to induce Cdk1 knockout. Starting from 24 h after

seeding, cells were incubated in 150 μL of assay medium [1:9 ratio of alamarBlue (BUF012B; AbD Serotec) to growth medium] for 4 h, and metabolic activity was quantified by measuring the fluorescence at 590 nm.

For MEF colony-formation assays, cells were first infected with retroviruses expressing the indicated constructs. At 48 h after infection, 10,000 cells were seeded in 10-cm dishes with or without 4-OHT and cultured for 8 d until colonies formed. Cells were fixed with ice-cold methanol and stained with 0.02% Giemsa solution (GS-500; Sigma) in ddH_2O until colonies were visible. Colony-formation assay for liver tumor cells were performed essentially the same way, except only 2,000 cells were plated and colonies were fixed after 6 d.

Silencing of Cdk2 expression in MEFs was achieved by infection of the cells with retroviral shRNA constructs as described previously (9). Loss of Cdk2 expression was confirmed by real-time PCR and Western blot analyses.

For senescence-associated β-gal staining, Cdk1 knockout was induced for 48 h before fixation and staining of the cells. Cells were washed two times with PBS and fixed for 5 min with 2% (wt/vol) formaldehyde/0.2% (wt/vol) glutaraldehyde solution in PBS. To visualize β-gal activity, cells were incubated overnight at 37 °C in staining solution [20 mM citric acid, 40 mM Na_2HPO_4 (pH 6.0), 150 mM NaCl, 5 mM potassium ferrocyanide, 5 mM potassium ferricyanide, 2 mM $MgCl_2$, 1 mg/mL X-Gal; 15520034; Invitrogen], and coverslips were mounted in Immu-Mount (9990402; Thermo Scientific) containing 2 μg/mL DAPI.

For BrdU labeling and FACS analysis, MEFs were grown to confluence in 15-cm dishes and serum starved for 72 h in 0.2% serum containing growth medium. To induce Cdk1 knockout, 20 ng/mL 4-OHT (H7904; Sigma) was added during the entire starvation period or only during the last 24 h. To induce synchronized entry into cell cycle, cells were trypsinized and replated in 10-cm dishes in full growth medium. To monitor S phase, cells were labeled with 100 μM BrdU (550891; BD Pharmingen) for 1 h before collection of the cells at different time points. At the end of each time point, cells were trypsinized and fixed in −20 °C cold 70% ethanol, stained with APC-conjugated anti-BrdU antibodies (623551; BD Pharmingen) and propidium iodide (81845; Sigma). Cell-cycle analysis was performed with a FACSCalibur flow cytometer (BD Biosciences), and resulting data were analyzed by FlowJo 8 software.

Partial Hepatectomy (PH) and Image Analysis. PH and BrdU labeling were performed as described (10, 11). For each time point, three or more animals were used, except the 72-h time point for $Cdk1^{FLOX/FLOX}$ mice, for which we used two animals. Animals were euthanized at the end of the time points, and livers were collected for further analysis by histology or immunoblotting. Histological sections were stained with mouse anti-BrdU antibodies (B35138; Invitrogen).

We developed custom software with an interactive user interface to detect, count, and measure nuclei in histological liver sections. The image analysis pipeline consists of seven steps. (*i*) The user selects representative points in two types of foreground regions (BrdU-positive nuclei in brown, BrdU-negative nuclei in blue) and background regions. To achieve a good sampling of the three image regions, the user should click multiple points of each color. (*ii*) The image is transformed from the RGB into the CIELAB color space. CIELAB was designed to provide a better model for human color perception than RGB (12). (*iii*) Based on similarity in the 3D CIELAB color space, each pixel in the image is classified according to the three user-defined image categories (background, unlabeled, or BrdU-labeled nuclei). (*iv*) After color segmentation, connected component analysis identifies the initial objects in the image foreground. (*v*) A series of postprocessing steps is applied to the foreground objects. Morphological operations such as closing and hole-filling restore object shapes. Shape filtering based on size and roundness helps to remove noise and distinguish between the nuclei of Kupffer cells and hepatocytes. Moreover, a cell-splitting algorithm (13) is applied to separate touching cells. (*vi*) Objects are classified as BrdU-labeled or unlabeled nuclei based on the majority of pixels corresponding to the respective category. (*vii*) Finally, statistics, including number, size, and density of the different types of nuclei, are computed and exported as Excel files. To improve productivity and reproducibility, user-defined parameters for color selection and postprocessing can be saved and reused for the analysis of other images. The software was implemented in Matlab (MathWorks) and is available upon request.

1. Truett GE, et al. (2000) Preparation of PCR-quality mouse genomic DNA with hot sodium hydroxide and tris (HotSHOT). *Biotechniques* 29:52–54.
2. Rodríguez CI, et al. (2000) High-efficiency deleter mice show that FLPe is an alternative to Cre-loxP. *Nat Genet* 25:139–140.
3. Lewandoski M, Meyers EN, Martin GR (1997) Analysis of Fgf8 gene function in vertebrate development. *Cold Spring Harb Symp Quant Biol* 62:159–168.
4. Postic C, Magnuson MA (2000) DNA excision in liver by an albumin-Cre transgene occurs progressively with age. *Genesis* 26:149–150.
5. Hayashi S, McMahon AP (2002) Efficient recombination in diverse tissues by a tamoxifen-inducible form of Cre: A tool for temporally regulated gene activation/inactivation in the mouse. *Dev Biol* 244:305–318.
6. Vooijs M, Jonkers J, Berns A (2001) A highly efficient ligand-regulated Cre recombinase mouse line shows that LoxP recombination is position dependent. *EMBO Rep* 2:292–297.
7. Bonin A, Reid SW, Tessarollo L (2001) Isolation, microinjection, and transfer of mouse blastocysts. *Methods Mol Biol* 158:121–134.
8. Berthet C, Aleem E, Coppola V, Tessarollo L, Kaldis P (2003) Cdk2 knockout mice are viable. *Curr Biol* 13:1775–1785.
9. Kozar K, et al. (2004) Mouse development and cell proliferation in the absence of D-cyclins. *Cell* 118:477–491.
10. Mitchell C, Willenbring H (2008) A reproducible and well-tolerated method for 2/3 partial hepatectomy in mice. *Nat Protoc* 3:1167–1170.
11. Satyanarayana A, Hilton MB, Kaldis P (2008) p21 Inhibits Cdk1 in the absence of Cdk2 to maintain the G1/S phase DNA damage checkpoint. *Mol Biol Cell* 19:65–77.
12. Dong G, Xie M (2005) Color clustering and learning for image segmentation based on neural networks. *IEEE Trans Neural Netw* 16:925–936.
13. Yu W, Lee HK, Hariharan S, Bu W, Ahmed S (2010) Evolving generalized Voronoi diagrams for accurate cellular image segmentation. *Cytometry A* 77:379–386.

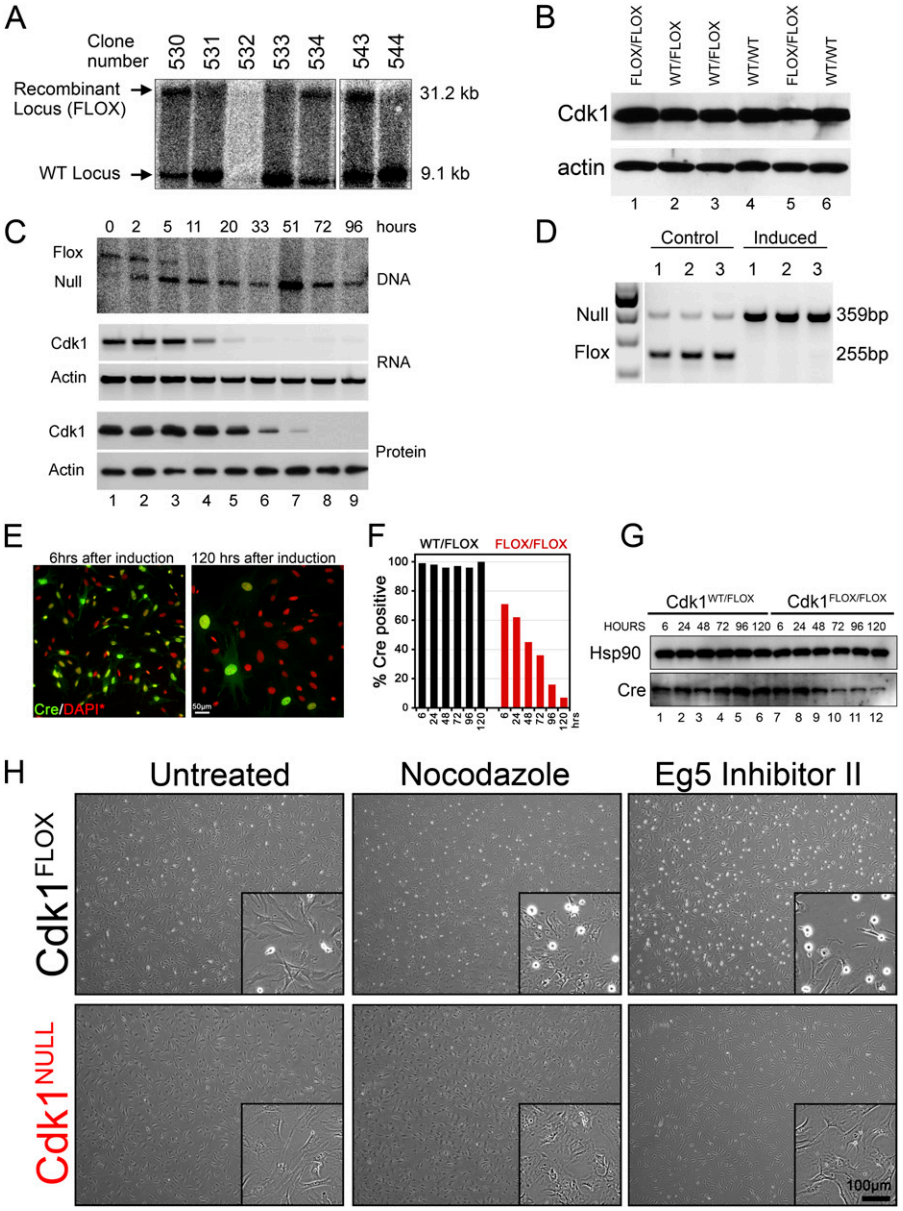

Fig. S1. Generation of the Cdk1 conditional knockout mice and induction of Cdk1 loss in MEFs. (*A*) Genomic DNA isolated from ES cell colonies was digested with EcoRV and analyzed by Southern hybridization using a 5′ probe (PKO0380/PKO0381, 399 bp). ES cell clones 530, 534, and 543 did undergo homologous recombination in the Cdk1 locus, which yields a 31.2-kb fragment because of the absence of the EcoRV site in targeted DNA. (*B*) Ten micrograms of protein extracts from passage 1 $Cdk1^{WT/WT}$ (lanes 4 and 6), $Cdk1^{WT/FLOX}$ (lanes 2 and 3), or $Cdk1^{FLOX/FLOX}$ (lanes 1 and 5) MEFs were analyzed by immunoblotting with antibodies against Cdk1 and actin, which serves as a loading control. Introduction of the LoxP recombination sites flanking exon 3 had no effects on Cdk1 protein expression levels or viability of the $Cdk1^{FLOX/FLOX}$ mice (data not shown). (*C*) To generate an inducible version of Cdk1 knockouts, $Cdk1^{FLOX}$ mice were mated with a transgenic line ubiquitously expressing Cre-Esr1 under the control of chicken β-actin promoter (1). Recombination between the LoxP sites can be induced by 4-OHT addition, which results in translocation of cytosolic Cre recombinase to the nucleus. Passage 1 MEFs of the $Cdk1^{FLOX/FLOX}$; $Cre\text{-}Esr1^{TG/TG}$ genotype were treated with 20 ng/mL of 4-OHT to induce Cdk1 knockout. DNA, RNA, and protein samples were collected at different time points after addition of 4-OHT and analyzed by Southern blot, RT-PCR, and Western blotting, respectively. Recombination at the Cdk1 locus is complete within 11 h, but it takes longer for the Cdk1 mRNA and protein to be degraded completely. (*D*) A complete Cdk1 knockout at protein level required more than 48 h in a growing MEF population during which time some cells will have lost Cdk1 earlier than others. For a more accurate comparison of $Cdk1^{NULL}$ and $Cdk1^{FLOX}$ MEFs, cells were synchronized to G0/G1 phase by serum starvation and simultaneously recombination was induced by 4-OHT for 72 h. PCR genotyping at the end of the starvation period demonstrated a complete knockout of the Cdk1 locus in the MEFs from three different embryos. (*E–G*) In our initial experiments to analyze the effects of Cdk1 loss in MEFs, we were not able to maintain MEF cultures with $Cdk1^{NULL/NULL}$ genotype when they expressed a single copy of the Cre-Esr1 transgene, i.e., $Cre\text{-}Esr1^{WT/TG}$. Detailed analyses (below) suggested that the MEF population with $Cdk1^{FLOX/FLOX}$ genotype lost Cre-expressing cells rapidly when induced with 4-OHT. For this reason, we always used homozygous $Cre\text{-}Esr1^{TG/TG}$ MEFs in all of the experiments described in this study. $Cdk1^{WT/FLOX}$ or $Cdk1^{FLOX/FLOX}$ MEFs heterozygous for Cre-Esr1 transgene ($Cre\text{-}Esr1^{TG/WT}$) were induced with 4-OHT and cultured for the indicated time points. Because loss of both copies of Cdk1 results in halt of cell division, cells that had previously lost Cre expression because of mutations, silencing, or DNA recombination possess a positive selection advantage. Coimmunostaining of cells with anti-Cre antibody (green) and DAPI (red; *pseudocolor) indicated a rapid loss of Cre-expressing $Cdk1^{FLOX/FLOX}$ ($Cdk1^{NULL/NULL}$) cells from the population (*E* and *F*). $Cdk1^{WT/FLOX}$ MEFs retain Cre expression (*F*). Western blot analysis indicated a reduction of Cre expression levels in induced $Cdk1^{FLOX/FLOX}$ MEF cells collected at the indicated time points after 4-OHT addition (*G*, lanes 7–12). $Cdk1^{WT/FLOX}$ MEFs retain a stable Cre expression level (*G*, lanes 1–6). (*H*) Passage 1 MEFs ($Cdk1^{FLOX/FLOX}$; $Cre\text{-}Esr1^{TG/TG}$) were synchronized by serum starvation for 72 h while Cdk1 knockout was induced

Legend continued on following page

simultaneously by the addition of 4-OHT during the last 24 h. Cells were released to enter cell cycle by plating them in growth medium with 10% serum and analyzed 30 h later by phase-contrast microscopy. Rounded up cells undergoing mitosis were visible with bright, spherical morphology (*Insets* in *Upper)*. To enrich for mitotic cells in the culture, MEFs were treated with mitosis-arresting drugs at 24 h after serum induction. Cells were left untreated (*Left*), treated with 0.5 μg/mL nocodazole (M1404; Sigma; *Center*), or 5 μM Eg5 kinesin inhibitor II (324621; Merck; *Right*). *Inset* magnification is fivefold higher than overview picture. (Scale bar: 100 μm.) In conclusion, $Cdk1^{NULL}$ MEFs were unable to initiate earlier events for mitotic entry such as modulation of actin cytoskeleton and rounding up of the cell body.

1. Hayashi S, McMahon AP (2002) Efficient recombination in diverse tissues by a tamoxifen-inducible form of Cre: A tool for temporally regulated gene activation/inactivation in the mouse. *Dev Biol* 244:305–318.

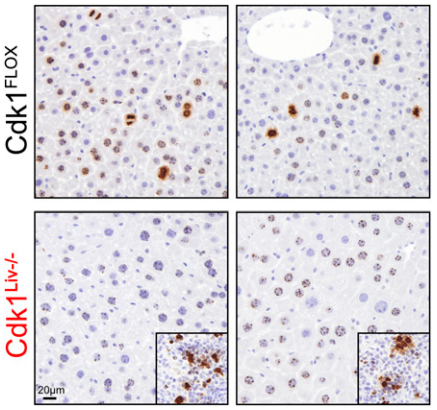

Fig. S2. Cdk1-deficient hepatocytes do not enter mitosis after PH. Seventy percent of $Cdk1^{FLOX}$ and $Cdk1^{Liv-/-}$ livers were removed by PH to induce entry of hepatocytes into cell cycle. At 48 h after PH, livers were isolated, and sections were stained with anti–phospho-histone H3 (Ser10) antibodies (06-570; Upstate Biotechnology) to monitor cells entering mitosis. Strongly stained mitotic cells are readily detectable in $Cdk1^{FLOX}$ (*Upper*) but not $Cdk1^{Liv-/-}$ (*Lower*) liver sections. *Insets* in the *Lower* show spleen sections from the same Cdk1 liver-knockout mice, and they were costained with the liver sections as a positive control. Two different animals were used for control and knockout sections.

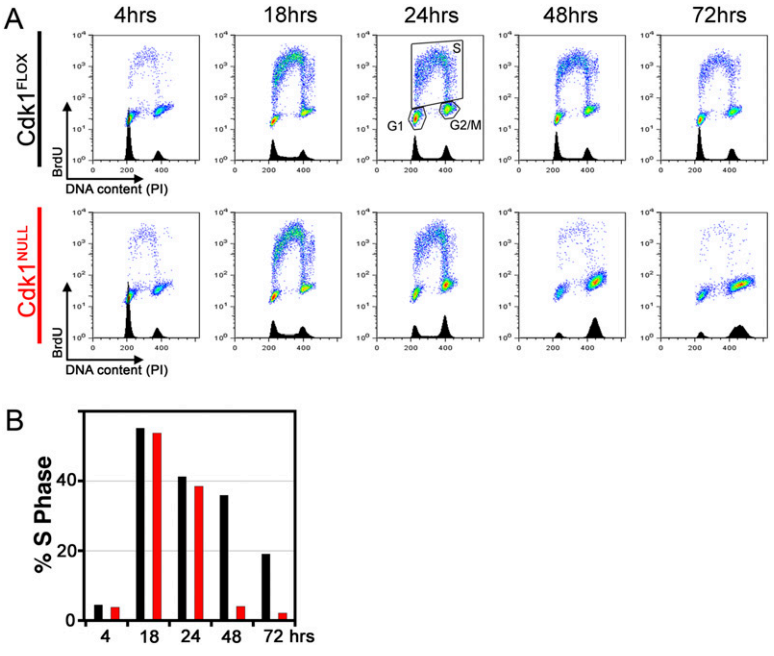

Fig. S3. FACS analysis. (*A* and *B*) Induction of Cdk1 knockout from the beginning of the serum starvation period resulted in accumulation of cells that had arrested at G2 phase, as well as cells with endoreduplicated (>4N) genomes, which also caused a slight reduction in percentage of cells in S phase at 18 and 24 h after serum stimulation (Fig. 3) because of the loss of Cdk1 before starvation-induced G0/G1 arrest. To refine our experimental system, we induced Cdk1 deletion only during the last 24 h of the serum starvation. Under these conditions, cells first become quiescent with G1 DNA content, and Cdk1 expression is down-regulated because of serum starvation. Addition of 4-OHT before serum stimulation ensures that new Cdk1 cannot be expressed because of deletion of the Cdk1 locus, which resulted in full Cdk1 knockout at the protein level. At 24 h, induction of Cdk1 knockout resulted in similar proportion of cells in G1, S, and G2 phases at 4-, 18-, and 24-h time points. Cells with endoreduplicated DNA content are not shown in *A*. Populations of cells in G1, S, and G2/M phases of the cell cycle were determined by dual-color FACS analysis using propidium iodide (to monitor DNA content) and APC-conjugated anti-BrdU antibodies (to monitor cells in S phase). With FlowJo 8 software, gates for G1, S, and G2/M phases were introduced, as illustrated for the 24-h time point in the first row of *A*, and the percentage of cells in each gate was quantified.

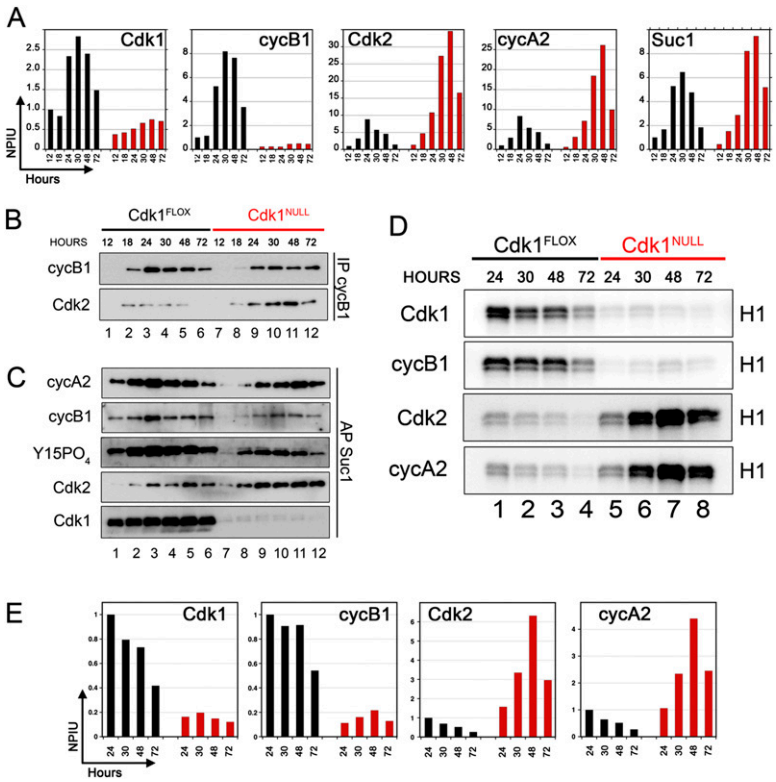

Fig. S4. Cdk activity assays in Cdk1-knockout MEFs. (*A*) Cdk1^{FLOX} MEFs were serum starved and simultaneously induced with 4-OHT for 72 h. Cells were released into the cell cycle by plating in medium with 10% serum and collected at the indicated time points for preparation of protein extracts. Cdks and cyclins were immunoprecipitated, and associated kinase activity against histone H1 was assayed as described in *SI Materials and Methods*. Graphs depict the quantitative analysis of the phosphorylated histone H1 in Fig. 4*A* using a phosphoimager. Histograms for Cdk1^{FLOX} MEFs are shown in black, and red was used to depict Cdk1^{NULL} histograms. (*B* and *C*) Protein extracts from Cdk1^{FLOX} and Cdk1^{NULL} MEFs collected at the indicated time points were used in immunoprecipitation assays with cyclin B1 antibodies or Suc1-decorated beads. Immunoprecipitated proteins were analyzed by Western blotting. In the absence of Cdk1, cyclin B1 was binding to Cdk2 (*B*, lanes 7–12), but this did not result in cyclin B1-associated kinase activity (*A*). Suc1 is a protein that binds to both Cdk1 and Cdk2 proteins (1). Affinity purification with Suc1-decorated beads followed by Western blot analysis suggested that the number of cyclin A2 molecules coprecipitated with Suc1 beads is unchanged between Cdk1^{FLOX} and Cdk1^{NULL} MEFs (*C*, first row). We can conclude that majority of cyclin A2 population is in complex with Cdk1 in Cdk1^{FLOX} MEFs and they completely switch into a complex with Cdk2 in Cdk1-deficient MEFs (Fig. 4). Comparison of cyclin B1 complexes (*C*, second row) suggests that a significant number of Cdk2/cyclin B1 complexes are forming in absence of Cdk1; however, these complexes are devoid of kinase activity (*A*, second chart). (*D* and *E*) Kinase assays were repeated under conditions where we induced the Cdk1 knockout only during the last 24 h of the serum-starvation period. Under these conditions, our major findings, i.e., accumulation of Cdk2 and cyclin A2-associated kinase activities, remain the same. Kinase activities were normalized to the first histogram in each chart (*A* and *E*). NPIU, normalized phosphoimager units.

1. Brizuela L, Draetta G, Beach D (1987) p13^{suc1} acts in the fission yeast cell division cycle as a component of the p34^{cdc2} protein kinase. *EMBO J* 6:3507–3514.

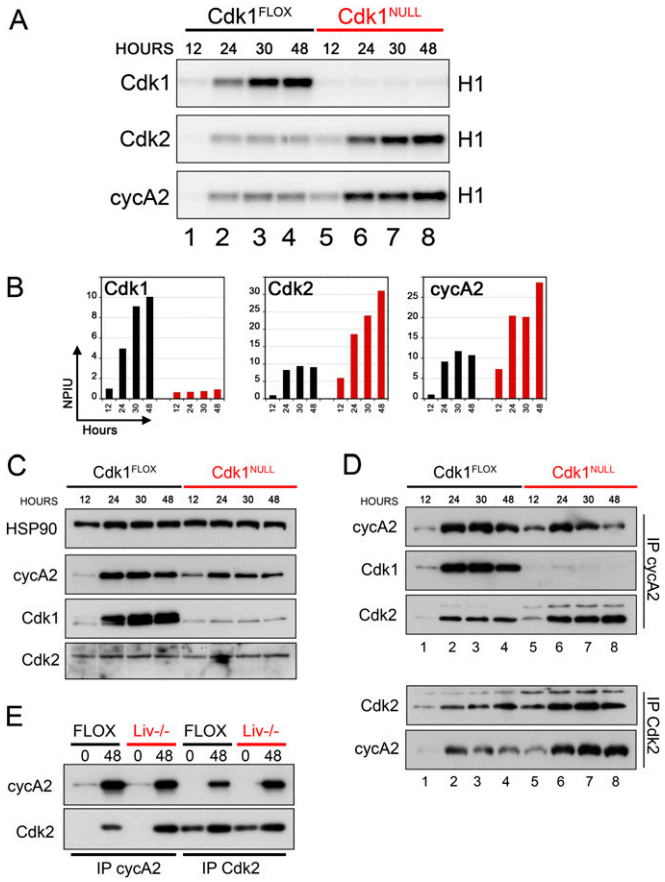

Fig. S5. Cdk activity assays in Cdk1-knockout liver tumor cells. (*A* and *B*) LI53 liver tumor cells (Fig. S9*B*) were treated essentially as explained above (Fig. S4*A*) to monitor accumulation of Cdk2 and cyclin A2-associated kinase activities upon Cdk1 knockout. (*C* and *D*) Protein extracts from $Cdk1^{FLOX}$ and $Cdk1^{NULL}$ liver tumor cells were collected at the indicated time points and analyzed with Western blot analysis (*C*) and immunoprecipitation assays using cyclin A2 and Cdk2 antibodies (*D*). Similar to experiments in MEFs (Fig. 4), we observe an accumulation of Cdk2/cyclin A2 complexes in Cdk1-knockout tumor cells, which explains the increased Cdk2 and cyclin A2-associated kinase activity in *A* and *B*. (*E*) To reproduce the results above (*A*–*D*) in a more physiological setting, we analyzed Cdk2/cyclin A2 complexes in $Cdk1^{FLOX}$ and $Cdk1^{Liv-/-}$ livers at 48 h after PH. Immunoprecipitation assays with either of Cdk2 or cyclin A2 demonstrated that there is an increase in Cdk2/cyclin A2 complexes upon Cdk1 knockout.

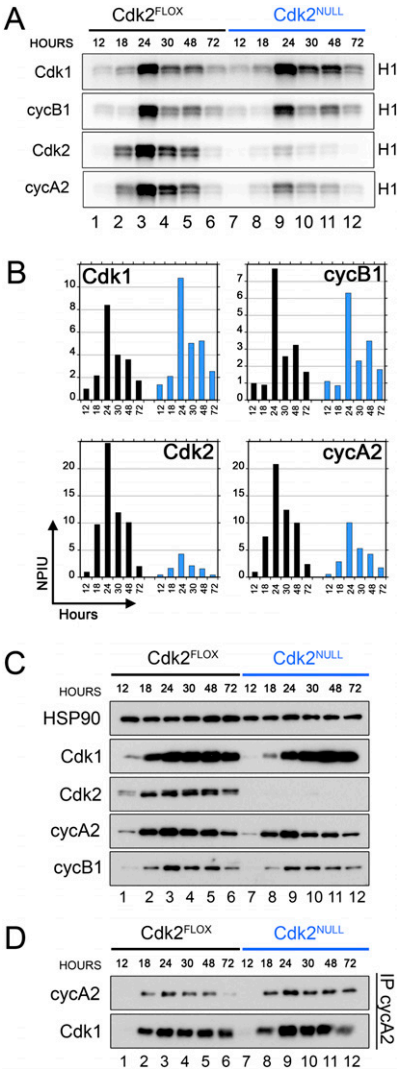

Fig. S6. Cdk activity assays in Cdk2-knockout MEFs. (*A* and *B*) Cdk2^{FLOX} MEFs were serum starved and simultaneously induced with 4-OHT for 72 h. Cells were released into the cell cycle by plating in growth medium with 10% serum and collected at the indicated time points for preparation of protein extracts. Cdks and cyclins were immunoprecipitated, and associated kinase activity against histone H1 was assayed (*A*) as described in *SI Materials and Methods*. Graphs (*B*) depict the quantitative analysis of the phosphorylated histone H1 in *A* by using a phosphoimager. Histograms from Cdk2^{FLOX} MEFs are shown in black, and blue is used to depict Cdk2^{NULL} histograms. We corroborated that Cdk1 and cyclin B1-associated kinase activities remain unchanged, whereas Cdk2-associated activity was depleted in Cdk2-deficient MEFs (1). Cyclin A2-associated kinase activity was significantly decreased (*B Lower Right*). (*C*) Western blot analysis of protein levels in Cdk2^{FLOX} and Cdk2^{NULL} MEFs indicated that Cdk1, cyclin A2, and cyclin B1 levels remained unchanged, whereas there was no Cdk2 expression in induced MEFs. Cdk1 expression was attenuated at 12 and 18 h after serum induction, as we reported earlier (1, 2), but remained comparable to controls at later time points. (*D*) When we analyzed the formation of complexes between Cdk1 and cyclin A2, we found slightly increased complexes in Cdk2^{NULL} MEFs. However, the cyclin A2-associated kinase activity was significantly lower, which corroborates that Cdk1/cyclin A2 complexes display decreased kinase activity compared with Cdk2/cyclin A2 (Fig. S8). Kinase activities were normalized to the first histogram in each chart. NPIU, normalized phosphoimager units.

1. Berthet C, Aleem E, Coppola V, Tessarollo L, Kaldis P (2003) Cdk2 knockout mice are viable. *Curr Biol* 13:1775–1785.
2. Ortega S, et al. (2003) Cyclin-dependent kinase 2 is essential for meiosis but not for mitotic cell division in mice. *Nat Genet* 35:25–31.

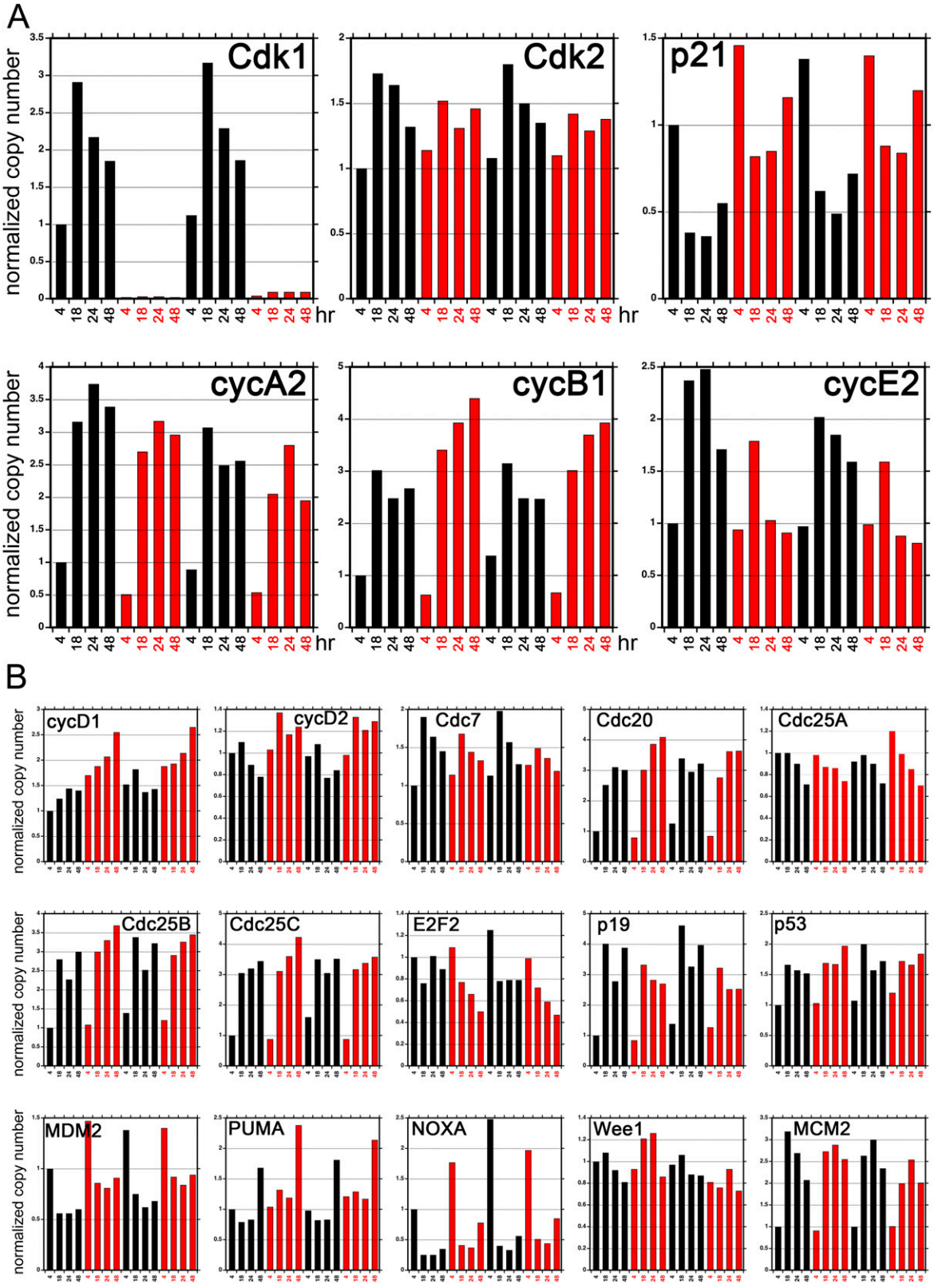

Fig. S7. mRNA expression analysis by RT-PCR. (*A* and *B*) To analyze the mRNA levels of different cell-cycle–associated genes, real-time PCR analysis was performed. To this effect, two independent clones of $Cdk1^{FLOX}$ MEFs were synchronized by serum starvation for 72 h while Cdk1 knockout was induced simultaneously by the addition of 4-OHT during the last 24 h. Cells were replated in presence of serum and collected at the indicated time points for RNA preparations. Real-time PCR analysis of RNA samples from $Cdk1^{FLOX}$ vs. $Cdk1^{NULL}$ indicated a complete loss of Cdk1 mRNA in the latter (*A Upper Left*). Cdk2, cyclin A2, and cyclin E2 expression levels were slightly decreased; in contrast, cyclin B1 and p21 levels were slightly increased upon Cdk1 loss (*A*). Cdk1 loss did not have any significant effects on the mRNA expression levels of other cell-cycle genes tested (*B*). All bars were normalized to the first one within the group.

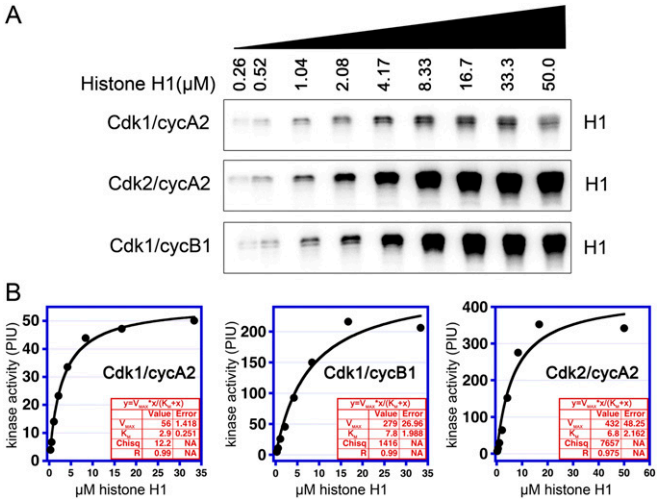

Fig. S8. Kinetic analysis of Cdk/cyclin complexes. (*A* and *B*) Purified Cdk/cyclin complexes were used in kinase assays where we varied the concentration of histone H1 as substrate. Phosphorylated histone H1 was separated by SDS/PAGE, and incorporated radioactive phosphate was measured at equal exposure times in a phosphoimager (*A*). K_m and V_{max} values were calculated and plotted by using the Michaelis–Menten enzyme kinetics template in the KaleidaGraph program (*B*).

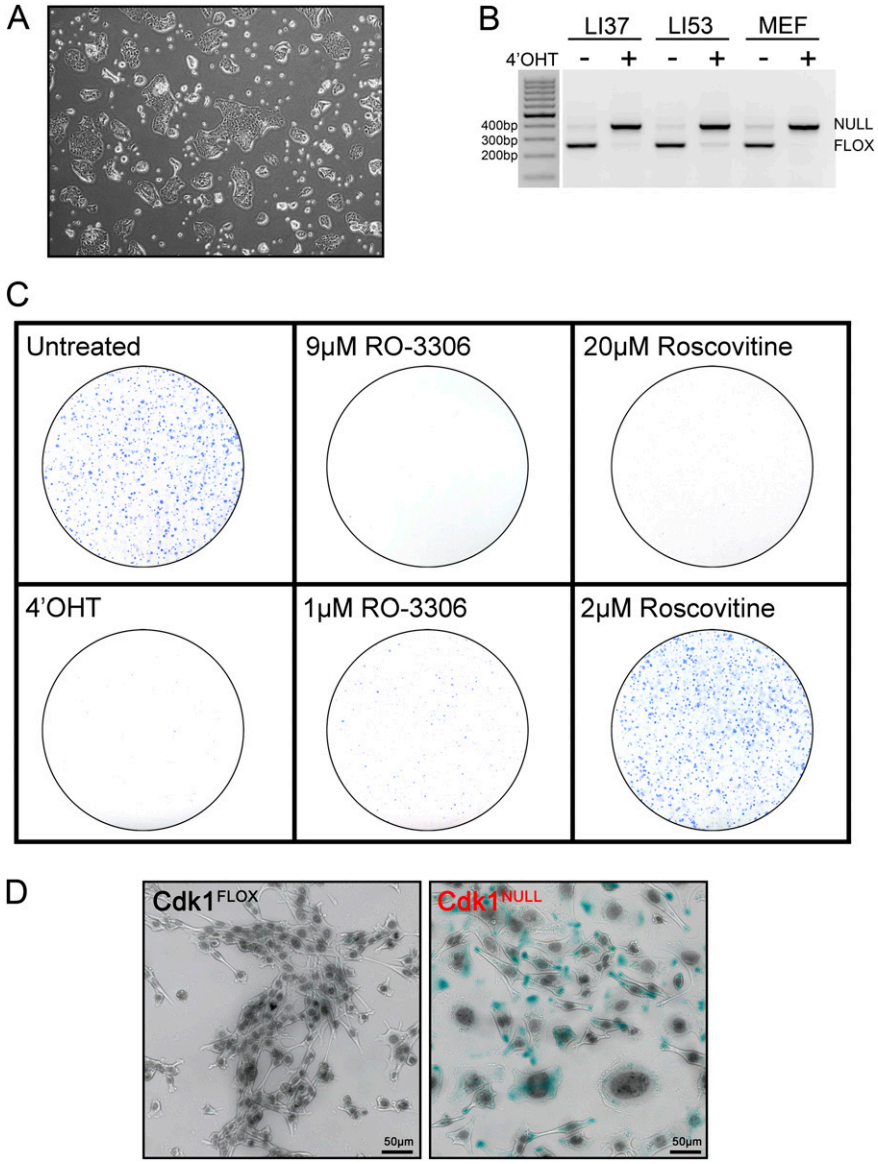

Fig. S9. Liver tumor cells cease proliferation and become senescent upon Cdk1 loss. (*A*) Liver tumors from two of the tail-vein–injected mice with Cdk1$^{FLOX/FLOX}$ genotype (LI37 and LI53) were isolated and dissociated to culture them in vitro. (*B*) These tumor cell lines were infected with a retroviral vector encoding the CreERT2 transgene so that they can be induced to undergo Cdk1 knockout. PCR genotyping is shown. (*C*) Induction of Cdk1 knockout by 4-OHT or addition of Cdk1 inhibitors RO-3306 (217699; Calbiochem) or roscovitine (557364; Calbiochem) to the culture medium prevented formation of colonies. Induction of Cdk1 knockout or inhibition of Cdk1 kinase activities by drugs prevented the proliferation of transformed hepatocytes, further confirming the essential role for Cdk1 in tumorigenesis. (*D*) Liver tumor cells were treated with 4-OHT to induce Cdk1 knockout. At 72 h after induction, senescent cells were monitored by senescence-associated β-gal staining, which yields a blue color. Essentially all Cdk1-deficient cells became senescent (*Right*), whereas untreated cells were not stained blue (*Left*).

Table S1. Primers for PCR genotyping of Cdk1

Primer name	Sequence (5′ → 3′)
Pr1 (PKO844)	TTTGTCAAGAAATGCAGCAGGACAC
Pr2 (PKO1158)	GCTCACATGTTCCTGAATGGTGGA
Pr3 (PKO1006)	GCGGTGGTTTAAACCCATAATCCCGGCAC

Table S2. Details of primers designed in house or purchased from SABiosciences

Gene name	Primer sequence (5′ → 3′) or source	Size, bp
Cdk1	GTCCGTCGTAACCTGTTGAG TGACTATATTTGGATGTCGAAG	215
Cdk2	GGGTCCATCAAGCTGGCAGA CCACAGGGTCACCACCTCAT	87
Cdc7	PPM03249E; SABiosciences	123
Cdc20	TTCCCAGGTGTGCTCCATCC CCCGTGCTGTGTGTCCTTTG	140
Cdc25a	PPM03246E; SABiosciences	93
Cdc25b	PPM03708A; SABiosciences	111
Cdc25c	PPM04967E; SABiosciences	86
cyclin A2	CAAGACTCGACGGGTTGCTC GCTGGCCTCTTCTGAGTCTC	144
cyclin B1	PPM02894E; SABiosciences	144
cyclin D1	PPM02903E; SABiosciences	172
cyclin D2	PPM02900E; SABiosciences	162
cyclin E2	PPM02904E; SABiosciences	99
Actin	ACGGCTCCGGCATGTGCAAA TTCCCACCATCACACCCTGG	105
Cyclophilin A	CCTTGGGCCGCGTCTCCTT CACCCTGGCACATGAATCCTG	147
E2F2	GCTGCCGGCCAAAAGGAAGT CTTGGGGGTTTTGGGGCTTG	121
Hsp90	ACTGCTCTGCTCTCCTCTGG CATCGATGCCCAGGCCTAGT	94
Mdm2	PPM02929B; SABiosciences	191
Puma	PPM04997A; SABiosciences	159
Noxa	PPM03403E; SABiosciences	191
Wee1	PPM04998E; SABiosciences	141
Mcm2	ATTTGAAGATGAGTCTGAGGGG CATCTTCATCATCCAGGGCCAA	161
p19	PPM02897A; SABiosciences	181
p21	PPM02901A; SABiosciences	153
p53	PPM02931A; SABiosciences	184